

## The Relationship of Modulation Generated in Brain Intrinsic Connectivity Networks by Simple Sensory Stimuli and Cognitive Performance

 Selen GÜR ÖZMEN<sup>1</sup>,  Emre HARI<sup>2,3</sup>,  Elif KURT<sup>3,4</sup>,  Hakan GÜRVI<sup>5</sup>,  Tamer DEMİRALP<sup>2,3</sup>

<sup>1</sup>Department of Physiotherapy and Rehabilitation, School of Health Sciences, Bahcesehir University, Istanbul, Türkiye

<sup>2</sup>Department of Physiology, Istanbul Faculty of Medicine, Istanbul University, Istanbul, Türkiye

<sup>3</sup>Hulusi Behcet Life Sciences Research Laboratory, Neuroimaging Unit, Istanbul University, Istanbul, Türkiye

<sup>4</sup>Department of Neuroscience, Aziz Sancar Institute of Experimental Medicine, Istanbul University, Istanbul, Türkiye

<sup>5</sup>Department of Neurology, Behavioral Neurology and Movement Disorders Unit, Istanbul Faculty of Medicine, Istanbul University, Istanbul, Türkiye

### ABSTRACT

**Introduction:** This study aimed to investigate the modulation of simple sensory stimuli on brain intrinsic connectivity networks in the Alzheimer's disease continuum (ADC) using functional magnetic resonance imaging (fMRI).

**Methods:** fMRI and neuropsychological assessment data of 88 cases in ADC were analysed. fMRI data were recorded in a session including blocks of light stimuli flickering at 20 Hz frequency and in the resting state from 21 Alzheimer's disease dementia (ADD), 34 mild cognitive impairment (MCI) and 33 subjective cognitive impairment (SCI). CONN (functional connectivity toolbox) software was used for functional connectivity analyses of fMRI data. Bonferroni correction was applied according to the number of ROIs in functional connectivity analyses and the significance threshold was determined as pFWE <0.0033.

**Results:** As a result of the analysis of the resting state data, decreased connectivity was detected between the posterior cingulate cortex seed of the default mode network and the temporal and parietal areas in ADD compared to the SCI and MCI groups. Decreased functional connectivity

was detected between the anterior insula and anterior cingulate cortex seeds of the salience network and the temporal, frontal and cingulate cortices in ADD compared to the SCI and MCI groups. However, in the data of flickering light stimulation at a frequency of 20 Hz, increased functional connectivity was detected between the right lateral prefrontal cortex seed of the frontoparietal network, which could not be captured with the resting state data, and the precuneus in the MCI group compared to the SCI group.

**Conclusions:** The increase in connectivity between the frontoparietal network and precuneus may be a compensatory response in the early stages of the disease. In addition, it was thought that fMRI images performed using simple sensory stimuli were more sensitive to cognitive decline in the early stages of the disease compared to resting state data and could have biomarker potential.

**Keywords:** Alzheimer's disease, functional magnetic resonance imaging, intrinsic connectivity networks, mild cognitive impairment, subjective cognitive impairment

**Cite this article as:** Gür Özmen S, Harı E, Kurt E, Gürvit H, Demiralp T. The Relationship of Modulation Generated in Brain Intrinsic Connectivity Networks by Simple Sensory Stimuli and Cognitive Performance. Arch Neuropsychiatry 2026;63:192–200. doi: 10.29399/npa.29010

### INTRODUCTION

Functional magnetic resonance imaging (fMRI) has revealed the existence of intrinsic connectivity networks (ICNs), which are crucial for understanding the brain's functional structure. These networks, particularly evident in resting-state fMRI, are essential for exploring brain dynamics across various states, including cognitive tasks (1). The resting state provides a standardised condition to study functional connectivity despite inherent variability due to physiological differences, highlighting the challenge of defining a universal baseline (1). Intrinsic connectivity networks can be broadly categorised into sensory-motor and cognitive networks, including the default mode network (DMN), salience network (SN), and others critical for complex cognitive functions.

The development of AD involves a gradual progression from subjective memory complaints to more severe stages of dementia, such as subjective cognitive impairment (SCI) and mild cognitive impairment (MCI). This progression emphasises the crucial role of early diagnosis, which can be facilitated by imaging studies that focus on ICNs (2).

### Highlights

- Functional connectivity has been studied in the Alzheimer's continuum.
- Simple sensory stimuli have the potential as biomarkers for early stages of dementia.
- Simple sensory stimuli are more sensitive to cognitive decline.

Studies have shown that individuals with AD exhibit decreased connectivity within the DMN, particularly in the posterior cingulate and hippocampal regions (3–5). Modifications in the connectivity patterns within the default mode network have been linked to the existence

of amyloid plaques, implying a straightforward association between alterations in the DMN and the underlying pathological processes of AD fMRI has the potential to shed light on the mechanisms of functional reorganisation in the brain's cortical and subcortical regions that occur as the disease progresses (6).

More recent studies have indicated that fMRI paradigms using either passive or simple active task conditions may be a more direct form of cognitive function assessment from resting-state recordings (5,7,8). That is especially true for patient groups such as AD dementia (ADD), or MCI where the use of complex task-based paradigms may have practical limitations in familiar compliance and cognitive load issues (9,10). Robust neural responses and ICN modulation using intrinsic connection networks (ICNs) can be evoked by simple sensory stimuli including periodic flashing light stimulation (10,11). Steady-state visually evoked potentials (SSVEPs) studies have shown that flickering light at particular frequencies can drive cortically synchronized oscillatory activity and hence provide a promising method to investigate functional connectivity changes in neurodegenerative diseases (7,12). In this context, there are studies indicating that 20 Hz stimulation is one of the most suitable frequencies to stimulate neural oscillatory mechanisms involved in cognitive processes (13,14). Functional connectivity between frontoparietal and default mode networks has been shown to be enhanced by 20 Hz flickering light stimulation in previous work; this suggests that the technique may have potential sensitivity towards mild cognitive impairment (MCI) prior to AD (8,14). Studies have also revealed that this frequency induces gamma-band activity, which is provocatively linked to attention, working memory and other higher-order cognitive functions (15). Therefore, in the spectrum of Alzheimer's disease, investigating the effects of easily applied and simple sensory stimuli, such as 20 Hz flicker light stimulation, on ICNs may contribute to current knowledge and provide new implications for the early diagnosis of the disease.

The primary goal of this research is to explore the effects of 20 Hz flickering light stimulation on ICNs and assess its potential role in enabling early detection of neurodegenerative diseases, particularly Alzheimer's disease. By analysing alterations in functional connectivity and their associations with cognitive measures, this research aims to improve diagnostic sensitivity.

## METHODS

### Participants

This study included 88 participants across the course of AD continuum, clinical and magnetic resonance imaging (MRI) data were collected between 2015 and 2017. Participants were grouped based on scores from the clinical dementia rating (CDR) scale and free and cued selective reminding test (FCSRT) (16–18). The AD dementia (ADD) group met NIA-AA clinical criteria, the diagnosis of MCI (FCSRT – total free recall score  $\leq 24$  and CDR score=0.5) in the study participants was established based on the diagnostic guidelines proposed by Petersen et al., and the SCI (FCSRT – total free recall score  $>24$  and CDR score=0) group had subjective memory complaints (19–21). The study was approved by the Clinical Research Ethics Committee of Istanbul University Istanbul Faculty of Medicine and conducted by the Declaration of Helsinki (Ethics Committee Decision No: 2018/710). Various tests were used to evaluate the detailed cognitive state of patients, including the Addenbrooke's Cognitive Examination Battery, Digit Span Forward, Stroop Test, Animal Naming Test, Backward Digit Span Test, Judgment of Line Orientation Test, Benton Facial Recognition Test, and Boston Naming Test.

### Magnetic Resonance Image Acquisition

Magnetic resonance imaging data was acquired at the Istanbul University Hulusi Behçet Life Sciences Research Laboratory. A Phillips Achieva 3

Tesla fMRI system, equipped with a 32-channel SENSE head coil, was employed for this purpose. To obtain high-resolution anatomical images weighted by T1, a 3D Turbo Field Echo (TFE) sequence was utilised. The imaging plane was axially oriented and aligned with the line connecting the anterior and posterior commissures. The acquisition parameters were set as follows: total scan duration of 4 minutes and 55 seconds, repetition time (TR) and echo time (TE) of 8.4 ms and 3.9 ms, respectively, flip angle of 8°, 180 axial slices with a thickness of 1 mm and no interslice gap, isotropic voxel size of 1 mm<sup>3</sup>, field of view (FOV) spanning 180 mm, and a data acquisition matrix measuring 220 × 240. The acquisition of functional MRI data relied on a T2\*-weighted echo-planar imaging (EPI) sequence. The imaging plane was axially oriented and aligned with the line connecting the anterior and posterior commissures. The acquisition parameters were set as follows: TR=3000 ms, TE=30 ms, flip angle of 80°, 48 axial slices, isotropic voxel size of 3.33 mm<sup>3</sup>, FOV spanning 212 × 198.75 mm, and an acquisition matrix measuring 64 × 59. During resting-state functional MRI, participants were instructed to remain awake, lie in a relaxed position with their eyes closed, and avoid focusing on any specific thoughts or stimuli. A total of 200 functional volumes were collected, resulting in a scan duration of 10 minutes.

Flashing light stimuli at a frequency of 20 Hz were used for task-based functional MRI. Stimuli were presented full-screen on a screen located on the back of the MRI machine using E-Prime software. Our stimulation frequency of 20 Hz was an exact divisor of our screen refresh rate of 60 Hz, so stimuli were reliably presented at the appropriate frequency. The stimulation sequence started with a baseline "off" period lasting 15 TRs. This was followed by three visual stimulation periods of 15 TRs each, interleaved with "off" periods of equal duration (15 TRs). During "off" periods, participants were instructed to focus on a fixation cross presented on a gray background. The scan session began with 10 dummy volumes to allow for signal stabilization, followed by the acquisition of 105 functional volumes, resulting in a total scan duration of 345 seconds.

### Magnetic Resonance Imaging Data Preprocessing

The data were pre-processed using SPM12 (Statistical Parametric Mapping, version 12) and the CONN functional connectivity toolbox version 20.b (22). Initially, functional images were realigned to the first volume to account for head motion. Subsequently, outlier scans were identified using the Artifact Detection Tools (ART) module integrated within CONN's preprocessing pipeline. Afterwards, functional and structural data were registered. Structural images were then segmented into grey matter, white matter (WM), and cerebrospinal fluid (CSF), and normalised to the Montreal Neurological Institute (MNI) standard space. The same transformation matrix was applied to the functional data, which were spatially normalised and resampled to isotropic voxels of 2 mm<sup>3</sup>. Finally, spatial smoothing was performed on the functional data using an isotropic Gaussian kernel with a full width at half maximum of 8 mm.

The functional data were denoised using the default pipeline provided by the CONN toolbox to reduce noise originating from motion and physiological effects. This process involved estimating noise components from WM and CSF signals, which were included as confounding variables during denoising. Additionally, six motion parameters (three translations and three rotations) obtained during the realignment step, their first-order derivatives, and outlier scans identified through the ART procedure were included as confounds. The effect of the scanning session was also modelled as a confounding factor. Finally, a temporal bandpass filter of 0.01–0.1 Hz was applied to the functional data.

### Functional Connectivity Analyses

Seed-to-voxel functional connectivity analysis was conducted using the CONN toolbox. Seeds from the default mode network (DMN), salience network (SN), and frontoparietal network (FPN), as defined in the network atlas provided by the CONN toolbox, were utilised for the analysis. The seeds for the DMN included the medial prefrontal cortex (MPFC), posterior cingulate cortex (PCC), and the right and left lateral parietal (LP) cortices. The seeds for the FPN consisted of the right and left lateral prefrontal cortices (LPFC) and posterior parietal cortices (PPC). The seeds for the SN comprised the anterior cingulate cortex (ACC), right and left anterior insulae (AI), rostral prefrontal cortices (RPF), and supramarginal gyri (SMG).

In the analyses, the main reason for focusing on the DMN, SN and FPN, which are amongst the three basic networks, is based on their critical roles in AD pathology and cognitive dysfunction. The fact that the DMN is one of the earliest networks affected in AD, the SN plays a critical role in attention functions and behaviour known to be affected in AD, and finally the role of the FPN in working memory and high-level cognitive functions are amongst the main reasons for focusing on these 3 networks (8,23,24).

For each subject, bivariate correlation coefficients were computed between the average time course of each seed region and the time courses of all other voxels in the brain. The resulting correlation coefficients were transformed into Z-scores using the Fisher transformation, which was subsequently used for second-level analyses.

F-tests were conducted to examine differences in resting-state functional connectivity (rs-FC) amongst the three groups. The voxel-based functional connectivity results were thresholded using an initial cluster-forming threshold of  $p < 0.001$  (uncorrected), followed by cluster-level thresholding at FWE (family-wise error)-corrected  $p < 0.05$ . These results were further Bonferroni corrected for multiple comparisons by adjusting the alpha level for the number of seeds (15),

resulting in a significance threshold of  $p_{FWE-corr} < 0.003$  (0.05/15). Post hoc two-sample t-tests were conducted for the seeds with significant F-test results. These tests were also thresholded using an initial cluster-forming threshold of  $p < 0.001$  (uncorrected) and cluster-level thresholding at FWE-corrected  $p < 0.05$ . Additionally, these results were further Bonferroni corrected for multiple comparisons by adjusting the alpha level for the number of groups (3), yielding a significance threshold of  $p_{FWE-corr} < 0.017$  (0.05/3).

### Statistical Analysis

Statistical tests were performed using IBM Statistical Package for Social Sciences (SPSS) program version 21 (IBM, Armonk, New York, United States). The Shapiro-Wilk normality test was used to test the normality of quantitative data distribution between groups. Depending on the distribution, independent sample t-tests or Mann-Whitney U tests were used for comparisons. On the other hand, one-way ANOVA was used to compare NPT scores among the three groups. The Pearson chi-square test was used for categorical variables. Finally, Pearson correlation analysis was performed to examine the relationship between memory scores and connectivity values in regions showing functional connectivity changes between groups. In the correlation analysis, functional connectivity values in anatomical regions where significant differences were detected as a result of ANOVA were included. Bonferroni correction was applied in the analyses and the significance threshold was determined as  $p=0.0125$  (0.05/4=0.0125).

## RESULTS

### Demographic and Clinical Results

There was no statistically significant difference between the groups in terms of demographic variables (Table 1). Comparisons of clinical data and post hoc analyses between the groups are presented in detail in Tables 1 and 2.

**Table 1.** Demographical data of the participants

	Mean and standard deviation.			Test	P value
	ADD (SD) [n=21]	MCI (SD) [n=34]	SCI (SD) [n=33]		
Age	67.4 (9.9)	63.7 (7.1)	63.1 (8.01)	0.153*	NS
Sex (F/M)	10/11	14/20	21/12	0.177 <sup>d</sup>	NS
Education	10.8 (4.6)	10.9 (4.9)	13.1 (4.7)	0.116*	NS
FCSRT-TFR	8.1 (7.2) [21]	18.3 (4.3) [34]	30.8 (4.4) [33]	126.633*	<0.001
FCSRT-cued	0.3 (0.2) [21]	0.6 (0.1) [34]	0.8 (0.1) [33]	42.063*	<0.001
Stroop interference	96.9 (79.6) [13]	57.1 (24.4) [34]	47.8 (21.0) [33]	7.750 <sup>i</sup>	<0.001
Animal counting	11.3 (4.3) [18]	16.9 (5.7) [34]	19.6 (5.1) [33]	14.369*	<0.001
Verbal fluency K-A-S	25.7 (14.7) [18]	31.7 (13.6) [34]	46.2 (16.5) [33]	12.919*	<0.001
Backward digit span	3.0 (0.6) [18]	3.8 (0.9) [34]	4.5 (0.8) [33]	29.002 <sup>i</sup>	<0.001
Forward digit span	5.2 (1.07) [18]	5.5 (0.8) [34]	5.6 (1.0) [33]	2.265 <sup>i</sup>	NS
Judgment of line orientation test	16.4 (6.7) [13]	20.0 (6.0) [34]	20.9 (4.6) [33]	5.261 <sup>i</sup>	NS
Benton face recognition test	42.3 (4.0) [21]	45.6 (3.9) [34]	47.9 (3.7) [33]	12.858*	<0.001
Boston naming test	27.3 (2.7) [18]	28.8 (2.0) [25]	30.3 (0.6) [18]	15.438 <sup>i</sup>	<0.001
Addenbrooke total	64 (13.5) [21]	80.5 (10.3) [34]	88.6 (6.6) [33]	38.555*	<0.001
Addenbrooke - MMSE	23.3 (3.7) [21]	27.9 (1.7) [34]	28.9 (1.3) [33]	37.315 <sup>i</sup>	<0.001
Addenbrooke - language	19 (4.5) [21]	21.8 (4.2) [34]	23.9 (2.2) [33]	15.824 <sup>i</sup>	<0.001
Addenbrooke - visual-spatial	12.3 (2.7) [21]	14.6 (1.4) [34]	15.2 (1.4) [33]	21.603 <sup>i</sup>	<0.001
Addenbrooke - attention	13.9 (2.1) [21]	17.2 (0.9) [34]	17.3 (1.2) [33]	36.735 <sup>i</sup>	<0.001
Addenbrooke - memory	10.4 (4.1) [21]	16.6 (4.7) [34]	20.1 (3.1) [33]	35.854*	<0.001
Addenbrooke - fluency	7.7 (3.2) [21]	10.0 (2.4) [34]	11.8 (2.0) [33]	23.703 <sup>i</sup>	<0.001

ADD: Alzheimer disease dementia; MCI: mild cognitive impairment; SCI: subjective cognitive impairment; SD: standard deviation; \*One-way ANOVA; <sup>i</sup>Kruskal Wallis H test; <sup>d</sup>Chi-square; The significance threshold was set as  $p < 0.05$ .

**Table 2.** Post hoc comparison results of clinical assessment scores between groups

	The p-values for pairwise comparisons		
	ADD and SCI	ADD and MCI	SCI and MCI
FCSRT- total free recall	<0.001	<0.001	<0.001
FCSRT- cued index	<0.001	<0.001	<0.001
Stroop interference	0.020	0.368	0.352
Animal counting	<0.001	0.002	0.112
Verbal fluency (K-A-S)	<0.001	0.517	0.001
Backward digit span	<0.001	0.004	0.029
Forward digit span	-	-	-
Judgment of line orientation test	-	-	-
Benton face recognition test	<0.001	0.011	0.057
Boston naming test	<0.001	0.189	0.054
Addenbrooke total	<0.001	<0.001	0.004
Addenbrooke – MMSE	<0.001	<0.001	0.540
Addenbrooke – language	<0.001	0.074	0.134
Addenbrooke – visual-spatial	<0.001	0.006	0.197
Addenbrooke – attention	<0.001	<0.001	1
Addenbrooke – memory	<0.001	<0.001	0.002
Addenbrooke – fluency	<0.001	0.060	0.013

ADD: Alzheimer's disease dementia; MCI: mild cognitive impairment; SCI: subjective cognitive impairment; MMSE: mini-mental state examination; Bonferroni correction was applied to the statistical results and the significance threshold was set at  $p < 0.05$ .

### Resting-state functional connectivity results

As a result of the resting state functional connectivity analysis performed between the three groups, significant differences were found in the functional connectivity of the salience network – anterior cingulate cortex, salience network – left anterior insula, salience network – right anterior insula, and default mode network (DMN) – posterior cingulate cortex regions of interest with various brain regions. Anatomical regions that showed changes in functional connectivity with DMN-PCC (default mode network-posterior cingulate cortex); right middle temporal gyrus-temporo – occipital part ( $p=0.003084$ ); Anatomical regions that showed changes in functional connectivity with SN-ACC (salience network-anterior cingulate cortex); right insular cortex, right central opercular cortex ( $p=0.000042$ ); Anatomical regions that showed changes in functional connectivity with left SN-AI (salience network-anterior insula) were anterior cingulate gyrus, bilateral supplementary motor cortex ( $p=0.000086$ ); and the anatomical regions that showed changes in functional connectivity with right SN-AI were anterior cingulate gyrus, right supplementary motor cortex ( $p=0.000083$ ). Detailed analysis results regarding group comparisons and post hoc comparisons in functional connectivity analyses are presented in Table 3.

### Results of Functional Connectivity Analysis of 20 Hz Light Stimulus

As a result of functional connectivity analysis performed on fMRI data recorded with 20 Hz light stimulation amongst the three groups, a statistically significant change in functional connectivity was detected between the FPN – right LPFC and precuneus ( $p=0.000212$ ). In post hoc comparisons, functional connectivity between FPN – right LPFC and precuneus increased in the MCI group compared to the SCI group ( $p=0.000030$ ). On the other hand, functional connectivity decreased in the ADD group compared to the MCI group ( $p=0.002269$ ) (Table 4).

### Results of Correlation Analysis Between Functional Connectivity Values and Memory Scores

As a result of the correlation analysis, it was determined that the regions showing connectivity changes with DMN and SN seeds were highly

correlated with memory scores. The correlation analysis findings are as follows: The functional connectivity changes between SN-ACC and right insular cortex and right central opercular cortex was positively correlated with FCSRT-total free recall scores ( $r=0.505$ ,  $p < 0.0001$ ); The functional connectivity changes between DMN-PCC and right middle temporal gyrus-temporo-occipital part was positively correlated with FCSRT-total free recall scores ( $r=0.318$ ,  $p=0.003$ ); The connectivity between left SN-AI and anterior cingulate gyrus and bilateral supplementary motor cortex was positively correlated with FCSRT-total free recall scores ( $r=0.547$ ,  $p < 0.0001$ ); The connectivity changes between right SN-AI and anterior cingulate gyrus and right supplementary motor cortex showed positive correlation with FCSRT-total free recall scores ( $r=0.580$ ,  $p < 0.0001$ ).

## DISCUSSION

Functional connectivity evaluates the integration of brain activity between distant brain regions, independent of structural connections. As a result of the functional connectivity analyses performed in our study, the default mode network and salience networks show a decrease in connectivity throughout the disease continuum (Figure 1-4). In addition, the high correlation between these functional connectivity changes and memory scores supports the critical effect of these networks on memory performance. However, these two networks, which were detected without any task and as a result of the analysis of the resting state data, do not have the sensitivity to distinguish between SCI and MCI groups. On the other hand, as a result of the analysis of fMRI recordings performed with 20 Hz light stimulation, FPN showed a significant increase in functional connectivity in the MCI stage of the disease and this increase was able to distinguish between SCI and MCI groups. In this context, a simple 20 Hz light stimulation increased the sensitivity to the early stages of the disease (Figure 5).

In the AD continuum, the PCC within the DMN shows functional connectivity changes. In the ADD group, functional connectivity between PCC and right middle temporal gyrus-temporo-occipital part, right posterior supramarginal gyrus, right angular gyrus, right

**Table 3.** The functional connectivity differences between groups

Region of interest	Contrast	MNI coordinate	Cluster size	Regions	P <sub>FWE</sub>
DMN - PCC	Group differences	+54, -48, -02	359	Right middle temporal gyrus-temporo-occipital part	0.003084
	ADD >MCI	+54, -48, -02	1549	Right middle temporal gyrus-temporo-occipital part, right supramarginal gyrus-posterior division, right angular gyrus, right planum temporale, right inferior temporal gyrus-temporo-occipital part	<0.001
	ADD >SCI	+60, -56, -08	514	Right middle temporal gyrus-temporo-occipital part, right inferior temporal gyrus-temporo-occipital part	0.002
SN-ACC	Group differences	+50, +06, -04	711	Right insular cortex, right central opercular cortex	0.000042
	ADD >MCI	+46, -04, +10	1213	Right insular cortex, right central opercular cortex, right frontal opercular cortex	<0.001
		+28, +16, -32	430	Right temporal pole	0.007
	ADD <SCI	+50, +06, -04	1802	Right insular cortex, right central opercular cortex, right putamen, right precentral gyrus, right frontal opercular cortex	<0.001
+46, -20, +12		812	Left insular cortex, left inferior frontal gyrus-pars opercularis	<0.001	
Left SN-AI	Group differences	+04, +06, +50	607	Anterior cingulate gyrus, right supplementary motor cortex, left supplementary motor cortex	0.000086
	ADD >MCI	+36, +12, +04	763	Right insular cortex	<0.001
		+12, +10, +40	430	Right paracingulate gyrus, anterior cingulate gyrus	0.003
	ADD >SCI	+02, +06, +50	1769	Anterior cingulate gyrus, right supplementary motor cortex, left supplementary motor cortex, right superior frontal gyrus, right paracingulate gyrus	<0.001
+04, +06, +48		348	Right frontal pole	<0.001	
Right SN-AI	Group differences	+04, +06, +48	611	Anterior cingulate gyrus, right supplementary motor cortex	0.000083
	ADD >MCI	-02, +28, +20	469	anterior cingulate gyrus, right paracingulate gyrus	0.003
	ADD >SCI	+06, +08, +46	1632	Anterior cingulate gyrus, right supplementary motor cortex, left supplementary motor cortex, right paracingulate gyrus	<0.001

ADD: Alzheimer's disease dementia; MCI: mild cognitive impairment; SCI: subjective cognitive impairment; FWE: family-wise error; MNI: Montreal Neurological Institute; DMN-PCC: default mode network-posterior cingulate cortex; SN-ACC: salience network-anterior cingulate cortex; SN-AI: salience network-anterior insula; Bonferroni correction was applied to the analysis results, and the significance threshold was set to  $p < 0.0033$  in group comparisons and  $p < 0.017$  in post hoc comparisons; regions with a voxel size of less than 100 were not reported.

**Table 4.** 20 Hz light stimulus functional connectivity results

Region of interest	Contrast	MNI coordinate	Cluster size	Regions	P <sub>FWE</sub>
Right FP - LPFC	Group differences	+12, -46, +06	349	Precuneus	0.000212
	ADD >MCI	+12, -46, +06	338	Precuneus	0,002269
	MCI >SCI	+12, -56, +08	614	Precuneus	0.000030

SCI: subjective cognitive impairment; MCI: mild cognitive impairment; ADD: Alzheimer's disease dementia; FWE: family-wise error; MNI: Montreal Neurological Institute; FP-LPFC: frontoparietal network - lateral prefrontal cortex; Bonferroni correction was applied to the analysis results, and the significance threshold was set to  $p < 0.0033$  in group comparisons and  $p < 0.017$  in post hoc comparisons; regions with a voxel size of less than 100 were not reported.

planum temporale decreased compared to the MCI group, while PCC and right middle temporal gyrus-temporo-occipital part and right inferior temporal gyrus-temporo-occipital part connectivity decreased compared to the SCI group. The DMN is the first and most consistently reported resting state network to be implicated in the pathophysiology of Alzheimer's disease (8). On the other hand, it has been reported that the disruption of the integrity of the DMN may be associated with the severity and progression of the clinical course in AD (25). One of the most fundamental hubs of the DMN is considered to be the PCC (26). The PCC is an area with higher metabolic activity in the brain and dense structural and functional connections with many brain regions. In addition, the PCC has been associated with cognitive functions known to be significantly affected in AD, such as episodic memory, attention, and emotion (27). In the AD continuum, PCC hypometabolism, atrophy, and decreased functional connectivity have been frequently reported in the literature (27,28). In addition, Berron et al. reported decreased functional connectivity between the medial temporal lobe and posterior-medial regions, predominantly the anterior hippocampus and PCC, in amyloid- $\beta$

pathology positive MCI group (29). In this context, the anatomical regions where PCC exhibits decreased functional connectivity are consistent with the regions involved in these functions.

In the study, salience network-related ACC and anterior insula seeds showed significant functional connectivity reduction with widespread cortical regions, especially frontal, temporal and cingulate cortices, in Alzheimer's disease continuity. However, no functional connectivity change was detected between SCI and MCI groups as a result of the analyses. The ACC has been associated with conflict monitoring, interference, response selection, sustained attention, decision making, social interactions, and empathy in the literature (9,30). Jeong et al. reported that the decrease in the thickness of the ACC may be an indicator of the transformation of amnesic-MCI to psychotic ADD (31). In this context, the probability of behavioural disorders in the Alzheimer's continuum is quite high, and apathy can be considered one of the most common neuropsychiatric symptoms of dementia (32). In addition, apathy has been associated with a worse prognosis in ADD (33). Neuroimaging studies have emphasised

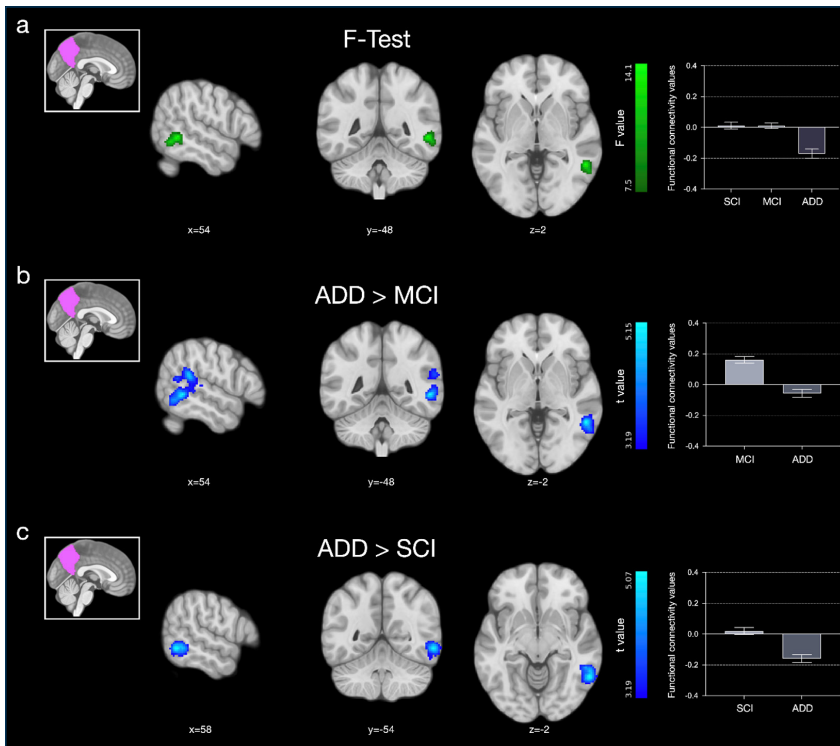


**Figure 1.** Functional connectivity alterations in the default mode network (DMN) – posterior cingulate cortex. Group-level functional connectivity differences in the DMN, highlighting changes in the posterior cingulate cortex (a). Post hoc comparisons showing connectivity variations among Alzheimer's disease dementia and Mild cognitive impairment groups (b). Post hoc comparisons showing connectivity variations among Alzheimer's disease dementia and subjective cognitive impairment groups (c). (ADD: Alzheimer's disease dementia; MCI: mild cognitive impairment; SCI: subjective cognitive impairment.)

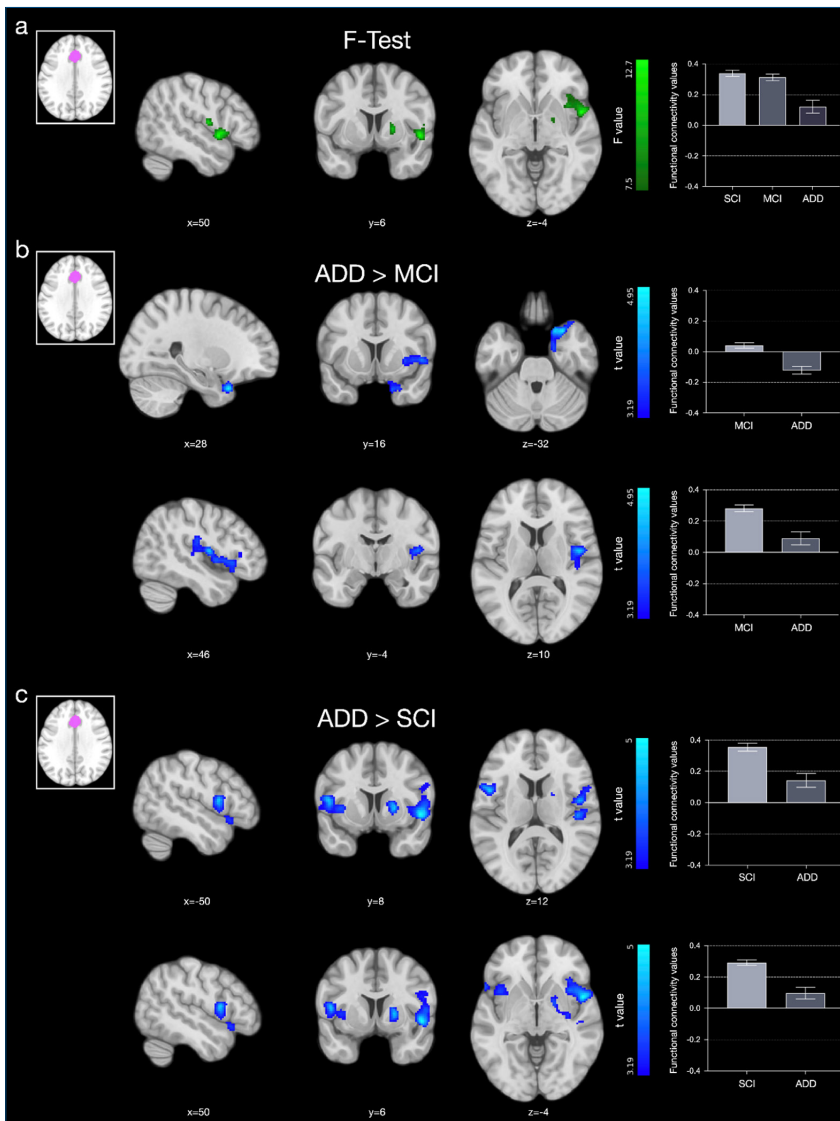


**Figure 2.** Functional connectivity alterations in the salience network (SN) – anterior cingulate cortex. Brain regions showing significant changes in anterior cingulate cortex connectivity (a). Post hoc comparisons showing connectivity variations among Alzheimer's disease dementia and Mild cognitive impairment groups (b). Post hoc comparisons showing connectivity variations among Alzheimer's disease dementia and subjective cognitive impairment groups (c). (ADD: Alzheimer's disease dementia; MCI: mild cognitive impairment; SCI: subjective cognitive impairment.)

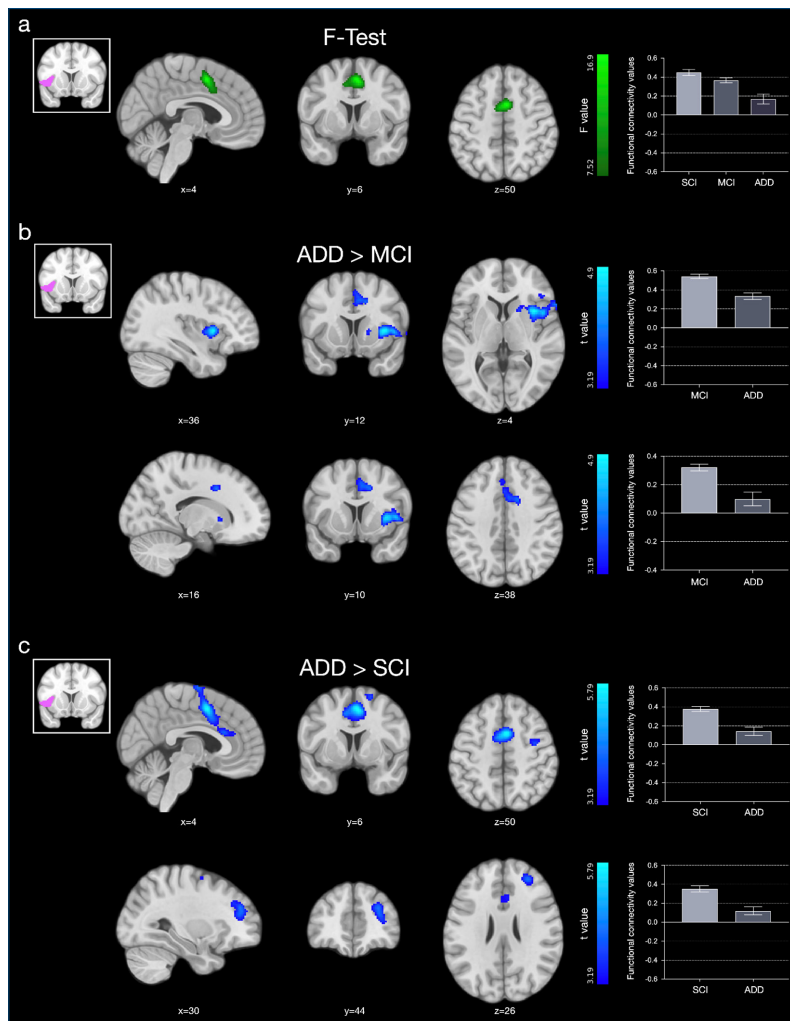


**Figure 3.** Functional connectivity alterations in the left salience network - anterior insula. Regions displaying altered connectivity with the left anterior insula (a). Post hoc comparisons showing connectivity variations among Alzheimer's disease dementia and Mild cognitive impairment groups (b). Post hoc comparisons showing connectivity variations among Alzheimer's disease dementia and subjective cognitive impairment groups (c). (ADD: Alzheimer's disease dementia; MCI: mild cognitive impairment; SCI: subjective cognitive impairment.)

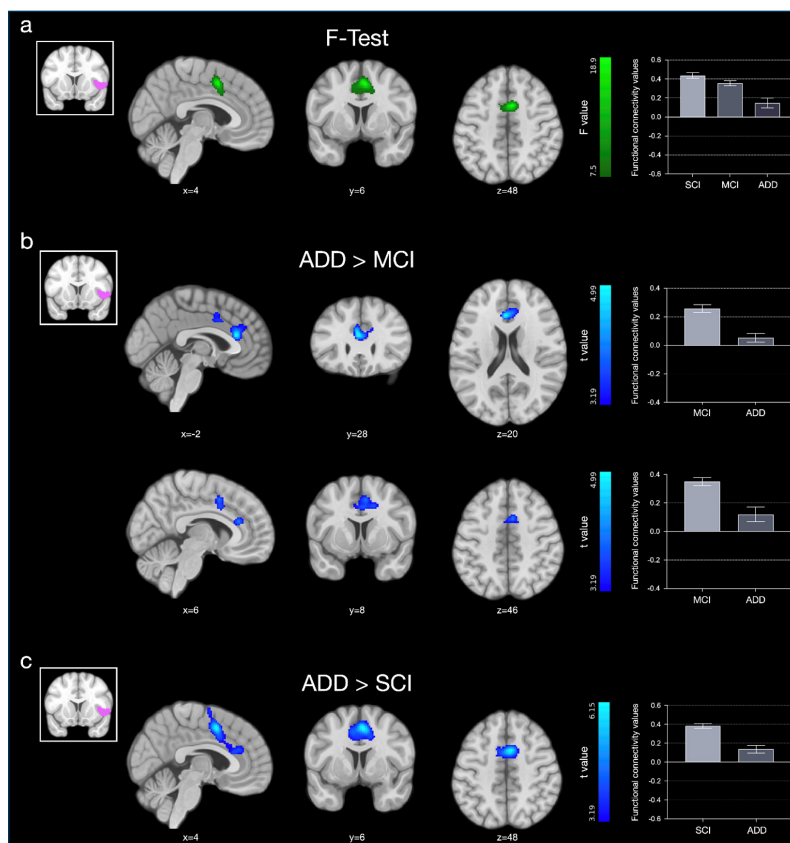


**Figure 4.** Functional connectivity alterations in the right salience network - anterior insula. Connectivity alterations in the right anterior insula across different stages of AD (a). Post hoc comparisons showing connectivity variations among Alzheimer's disease dementia and Mild cognitive impairment groups (b). Post hoc comparisons showing connectivity variations among Alzheimer's disease dementia and Subjective cognitive impairment groups (c). (ADD: Alzheimer's disease dementia; MCI: mild cognitive impairment; SCI: subjective cognitive impairment.)

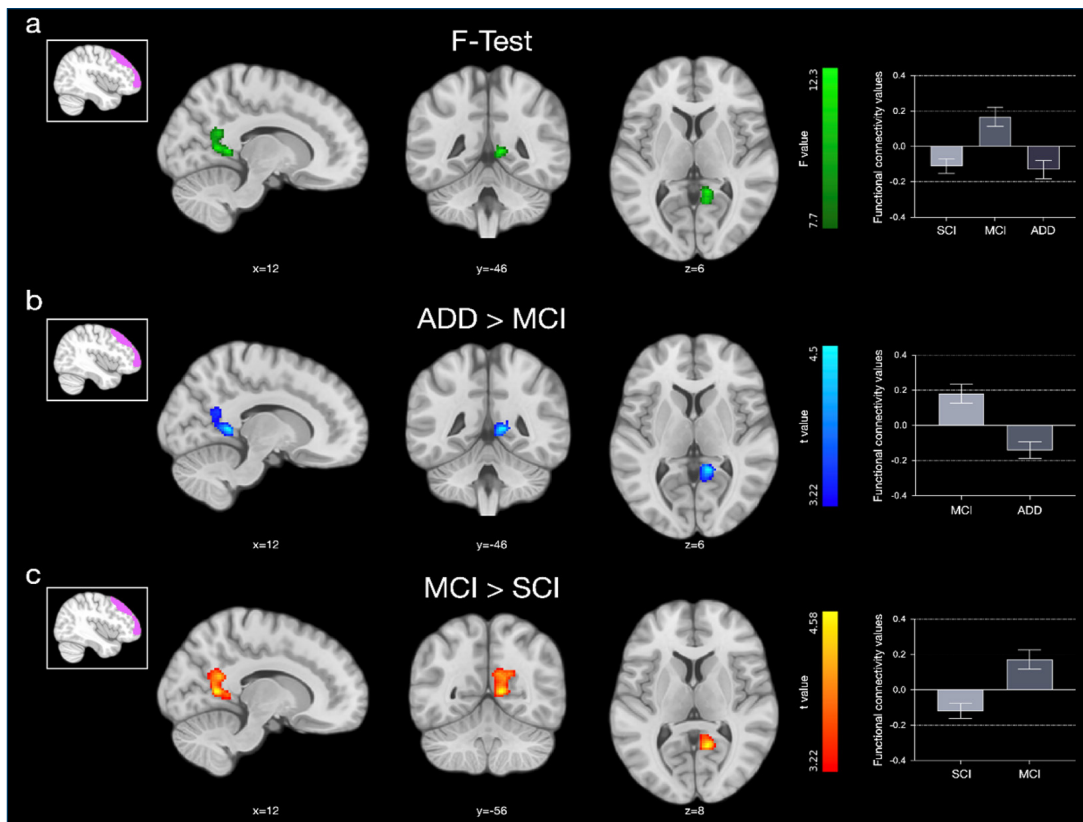


**Figure 5.** Effects of 20 Hz light stimulation on the frontoparietal network (FPN) – right lateral prefrontal cortex. Functional connectivity changes in the right lateral prefrontal cortex under 20 Hz stimulation (a). Post hoc comparisons showing connectivity variations among Alzheimer's disease dementia and Mild cognitive impairment groups (b). Post hoc comparisons showing connectivity variations among Mild cognitive impairment and Subjective cognitive impairment groups (c). (ADD: Alzheimer's disease dementia; MCI: mild cognitive impairment; SCI: subjective cognitive impairment).

that apathy occurs as a result of functional connectivity changes between fronto-striatal and limbic regions (33). In our study, the decrease in functional connectivity of the ACC with the anatomical regions mentioned above in ADD compared to MCI and SCI may contribute to the development of clinical apathy progressing to dementia. The lack of specific scales selected for the assessment of apathy in the study can be considered amongst the limitations of the study. However, the increase in Stroop interference from SCI to ADD for the assessment of frontal lobe functions in the study and the decrease in Animal Counting and K-A-S scores from SCI to ADD support the dysfunction in executive functions and its reflections on functional connectivity.

As a result of MRI data analysis related to 20 Hz light stimulation, a change in connectivity was detected between the lateral prefrontal cortex and precuneus belonging to the FPN. The change in connectivity between these anatomical regions showed an increase in the MCI stage of the disease and decreased again in the ADD stage. This observed increase was thought to be a compensatory increase against neurodegeneration in the course of the disease. The LPC plays a vital role in higher-level behavioral control through its rich anatomical connections with cortical association regions and subcortical structures. The executive functions mediated by this brain region can be conceptualized as distinct but interactive processes that work together to produce goal-directed behaviour in an integrated manner (34). Although the precuneus has been described as part of the DMN, studies have reported that the precuneus correlates with the DMN during resting states and with the FPN during tasks (35). In this context, our findings support the idea that the precuneus interacts with both networks.

Sensory functional brain networks can be investigated using periodic stimulation in steady-state paradigms. Studies using electrophysiological techniques have demonstrated that steady-state visually evoked potentials (SSVEP), elicited by periodic stimulation, exhibit a high signal-to-noise ratio and a consistent spectrum. These SSVEP responses can be triggered by visual stimuli with oscillation frequencies spanning from 4 to 75 Hz (11,12). We used light stimulation with a 20 Hz oscillation frequency in the present study. According to research findings, steady-state visual evoked potentials (SSVEPs) are generated from several distinct regions of the cerebral cortex, encompassing areas such as the parietal, temporal, frontal, and prefrontal lobes (7,10). Furthermore, the physical properties of the stimuli can influence the functional networks involving these regions (7). The amplitude, phase, and spatial distribution of SSVEP responses depend on the oscillation frequencies of the stimuli, suggesting that different frequencies may engage functionally distinct brain networks. The finding of connectivity changes between the right LPC and the precuneus had not been previously detected in resting-state functional connectivity. The detection of this finding with 20 Hz light stimulation appears significant as an fMRI finding and may hold potential as a biomarker for future similar studies.

Although our study was meticulously designed, there are several limitations. First, due to the nature of the disease, the average age of our dementia group is higher than the other two groups and the average education level is lower than the other two groups. The second limitation may be that the group numbers are not equal. As a solution to these limitations, conservative statistical corrections were applied in our study and the reliability of the findings was aimed to be increased.

In conclusion, our study provides valuable insights into functional connectivity changes associated with dementia. It supports that changes in functional connectivity patterns in the SN and DMN are associated with the performance of individuals on assessments measuring memory, attention processes, and executive functions in the Alzheimer's disease spectrum. Furthermore, a difference was detected between the early stages of the disease that were not detected at rest using 20 Hz flickering light stimulation. This finding emphasizes the importance of simple sensory stimuli for early detection of the disease.

**Acknowledgements:** We thank Burak Acar, Elif Yıldırım and Ezgi Soncu Büyüksan for their contribution

**Ethics Committee Approval:** The study was approved by the Clinical Research Ethics Committee of Istanbul University Istanbul Faculty of Medicine and conducted by the Declaration of Helsinki (Ethics Committee Decision No: 2018/710).

**Informed Consent:** All participants provided written informed consent.

**Peer-review:** Externally peer-reviewed.

**Author Contributions:** Concept- SGO, TD, EH, HG; Design- SGO, TD, EH, HG; Supervision- SGO, TD, HG; Data Collection and/or Processing- SGO, EH, EK; Analysis and/or Interpretation- SGO, TD, HG, EH; Literature Search- SGO, TD; Writing- SGO, TD, EH, EK, HG; Critical Reviews- HG, TD.

**Conflict of Interest:** The authors declared that there is no conflict of interest.

**Financial Disclosure:** Authors declared no financial support.

## REFERENCES

- Wang L, Zang Y, He Y, Liang M, Zhang X, Tian L, et al. Changes in hippocampal connectivity in the early stages of Alzheimer's disease: evidence from resting state fMRI. *Neuroimage*. 2006;31:496–504. [Crossref]
- Andrews-Hanna JR, Reidler JS, Sepulcre J, Poulin R, Buckner RL. Functional-anatomic fractionation of the brain's default network. *Neuron*. 2010;65:550–562. [Crossref]
- Rokicki J, Li L, Imabayashi E, Kaneko J, Hisatsune T, Matsuda H. Daily carnosine and anserine supplementation alters verbal episodic memory and resting state network connectivity in healthy elderly adults. *Front Aging Neurosci*. 2015;7:219. [Crossref]
- Hari E, Kurt E, Ulasoglu-Yildiz C, Bayram A, Bilgic B, Demiralp T, et al. Morphometric analysis of medial temporal lobe subregions in Alzheimer's disease using high-resolution MRI. *Brain Struct Funct*. 2023;228:1885–1899. [Crossref]
- Hari E, Kizilates-Evin G, Kurt E, Bayram A, Ulasoglu-Yildiz C, Gurvit H, et al. Functional and structural connectivity in the Papez circuit in different stages of Alzheimer's disease. *Clin Neurophysiol*. 2023;153:33–45. [Crossref]
- Brier MR, Thomas JB, Snyder AZ, Benzinger TL, Zhang D, Raichle ME, et al. Loss of intranetwork and internetwork resting state functional connections with Alzheimer's disease progression. *J Neurosci*. 2012;32:8890–8899. [Crossref]
- Srinivasan R, Fornari E, Knyazeva MG, Meuli R, Maeder P. fMRI responses in medial frontal cortex that depend on the temporal frequency of visual input. *Exp Brain Res*. 2007;180:677–691. [Crossref]
- Badhwar A, Tam A, Dansereau C, Orban P, Hoffstaedter F, Bellec P. Resting-state network dysfunction in Alzheimer's disease: a systematic review and meta-analysis. *Alzheimers Dement (Amst)*. 2017;8:73–85. [Crossref]
- Etkin A, Egner T, Kalisch R. Emotional processing in anterior cingulate and medial prefrontal cortex. *Trends Cogn Sci*. 2011;15:85–93. [Crossref]
- Vialatte F-B, Maurice M, Dauwels J, Cichocki A. Steady-state visually evoked potentials: focus on essential paradigms and future perspectives. *Prog Neurobiol*. 2010;90:418–438. [Crossref]
- Wu C-H, Chang H-C, Lee P-L, Li K-S, Sie J-J, Sun C-W, et al. Frequency recognition in an SSVEP-based brain computer interface using empirical mode decomposition and refined generalized zero-crossing. *J Neurosci Methods*. 2011;196:170–181. [Crossref]
- Zhang Y, Xu P, Huang Y, Cheng K, Yao D. SSVEP response is related to functional brain network topology entrained by the flickering stimulus. *PLoS One*. 2013;8:e72654. [Crossref]
- Buschman TJ, Miller EK. Top-down versus bottom-up control of attention in the prefrontal and posterior parietal cortices. *Science (1979)*. 2007;315:1860–1862. [Crossref]
- Herrmann CS, Strüber D, Helfrich RF, Engel AK. EEG oscillations: from correlation to causality. *Int J Psychophysiol*. 2016;103:12–21. [Crossref]
- Buzsáki G, Wang X-J. Mechanisms of gamma oscillations. *Annu Rev Neurosci*. 2012;35:203–225. [Crossref]
- Buschke H. Cued recall in amnesia. *J Clin Neuropsychol*. 1984;6:433–440. [Crossref]
- Morris JC. The clinical dementia rating (CDR): Current version and scoring rules. *Neurology*. 1993;43:2412–2412-a. [Crossref]
- Ivnik RJ, Smith GE, Lucas JA, Tangalos EG, Kokmen E, Petersen RC. Free and cued selective reminding test: MOANS norms. *J Clin Exp Neuropsychol*. 1997;19:676–691. [Crossref]
- Petersen RC. Mild cognitive impairment as a diagnostic entity. *J Intern Med*. 2004;256:183–194. [Crossref]
- Grober E, Sanders AE, Hall C, Lipton RB. Free and cued selective reminding identifies very mild dementia in primary care. *Alzheimer Dis Assoc Disord*. 2010;24:284–290. [Crossref]
- McKhann GM, Knopman DS, Chertkow H, Hyman BT, Jack CRJ, Kawas CH, et al. The diagnosis of dementia due to Alzheimer's disease: recommendations from the National Institute on Aging-Alzheimer's Association workgroups on diagnostic guidelines for Alzheimer's disease. *Alzheimers Dement*. 2011;7:263–269. [Crossref]
- Whitfield-Gabrieli S, Nieto-Castanon A. Conn: a functional connectivity toolbox for correlated and anticorrelated brain networks. *Brain Connect*. 2012;2:125–141. [Crossref]
- Greicius MD, Srivastava G, Reiss AL, Menon V. Default-mode network activity distinguishes Alzheimer's disease from healthy aging: evidence from functional MRI. *Proc Natl Acad Sci U S A*. 2004;101:4637–4642. [Crossref]
- Seeley WW, Crawford RK, Zhou J, Miller BL, Greicius MD. Neurodegenerative diseases target large-scale human brain networks. *Neuron*. 2009;62:42–52. [Crossref]
- Zhang H-Y, Wang S-J, Liu B, Ma Z-L, Yang M, Zhang Z-J, et al. Resting brain connectivity: changes during the progress of Alzheimer disease. *Radiology*. 2010;256:598–606. [Crossref]
- Raichle ME, MacLeod AM, Snyder AZ, Powers WJ, Gusnard DA, Shulman GL. A default mode of brain function. *Proc Natl Acad Sci U S A*. 2001;98:676–682. [Crossref]
- Leech R, Sharp DJ. The role of the posterior cingulate cortex in cognition and disease. *Brain*. 2014;137:12–32. [Crossref]
- Lee P-L, Chou K-H, Chung C-P, Lai T-H, Zhou JH, Wang P-N, et al. Posterior cingulate cortex network predicts Alzheimer's disease progression. *Front Aging Neurosci*. 2020;12:608667. [Crossref]
- Berron D, van Westen D, Ossenkoppelle R, Strandberg O, Hansson O. Medial temporal lobe connectivity and its associations with cognition in early Alzheimer's disease. *Brain*. 2020;143:1233–1248. [Crossref]
- Fan J, Hof PR, Guise KG, Fossella JA, Posner MI. The functional integration of the anterior cingulate cortex during conflict processing. *Cereb Cortex*. 2008;18:796–805. [Crossref]
- Jeong H-J, Lee Y-M, Park J-M, Lee B-D, Moon E, Suh H, et al. Reduced thickness of the anterior cingulate cortex as a predictor of amnesic-mild cognitive impairment conversion to Alzheimer's Disease with psychosis. *J Alzheimers Dis*. 2021;84:1709–1717. [Crossref]
- Marin RS. Apathy: concept, syndrome, neural mechanisms, and treatment. *Semin Clin Neuropsychiatry*. 1996;1:304–314. [Crossref]
- Azocar I, Rapaport P, Burton A, Meisel G, Orgeta V. Risk factors for apathy in Alzheimer's disease: a systematic review of longitudinal evidence. *Ageing Res Rev*. 2022;79:101672. [Crossref]
- Tanji J, Hoshi E. Role of the lateral prefrontal cortex in executive behavioral control. *Physiol Rev*. 2008;88:37–57. [Crossref]
- Utevsky AV, Smith DV, Huettel SA. Precuneus is a functional core of the default-mode network. *J Neurosci*. 2014;34:932–940. [Crossref]